Explicit filtering and subgrid-scale models in turbulent channel flow

By Jessica Gullbrand

1. Motivation and objectives

In large eddy simulation (LES), the large energy carrying length scales of turbulence are resolved and the small structures are modeled. The separation of large and small scales is done by applying a low-pass filter to the Navier-Stokes equations. The effect of the small-scale turbulence on the resolved scales is modeled using a subgrid-scale (SGS) model.

It is of great importance that the resolved length scales are captured accurately by the numerical scheme. Information from the smallest resolved length scales are commonly used to model the stresses of the unresolved scales in the SGS model. This requires that the numerical error of the scheme is sufficiently small. Therefore, high order numerical schemes are necessary in LES.

One approach is to use high-order finite-difference schemes. However, all finite-difference schemes have a truncation error that increases with the wavenumber (Lund & Kaltenbach 1995). To reduce the influence of this error, an explicit filtering can be applied that reduces or removes the small scales that otherwise would be largely affected by this error.

In using explicit filtering, it is a requirement that the filtering operation and the differentiation do commute. This is generally not the case in inhomogeneous flow fields where the required smallest resolved length scales vary throughout the flow fields. The varying filter width introduces a commutation error of $O(\Delta^2)$ where Δ represents the filter width (Ghosal 1996; Ghosal & Moin 1995). Therefore, most of the explicit filtering procedures that have been applied so far have been used in homogeneous flow fields or in homogeneous directions of more general flows. Explicit filtering in two dimensions has been studied by Lund & Kaltenbach (1995) and numerous filter functions by Piomelli *et al.* (1988) and Najjar & Tafti (1996).

The problem of lacking robust and straightforward filtering procedures that do commute was addressed by Vasilyev *et al.* (1998). They developed a general theory of discrete filtering for LES in complex geometries. A set of rules for constructing discrete filters, so that the filters commute to the desired order, was also proposed.

The ultimate goal of the explicit filtering procedure is to perform a "true" LES. In a true LES, the filtering procedure is decoupled from the computational grid. As the grid is refined while the explicit filter width is held fixed, the solution converges to a true LES. In the commonly-used approach to LES, the computational grid together with the low pass characteristics of the discrete differencing operators act as a filter and, as the grid is refined, the solution converges towards a direct numerical simulation (DNS) not an LES. However, before a true LES can be performed, the influence of the explicit filtering procedure on the SGS models need to be determined.

In this paper, explicit filtering is applied in three dimensions in a turbulent channel flow using the dynamic Smagorinsky model (DSM) (Germano *et al.* 1991) and the mixed model (MM) (Bardina *et al.* 1980; Zang *et al.* 1993) as SGS models. The turbulent

channel flow of Reynolds number $Re_\tau = 395$ is simulated using a conservative fourth-order finite-difference scheme (Vasilyev 2000). The influence of the three-dimensional filtering procedure on the DSM and the MM is investigated, as well as the influence of resolving the Leonard stress tensor. The results are compared to the DNS data by Moser *et al.* (1999).

2. Numerical method

2.1. *Governing equations*

In LES, the governing equations are filtered in space. The filter function G is applied to the flow variable f

$$\overline{f}(x,\Delta,t) = \int_{-\infty}^{\infty} G(x,x',\Delta) f(x',t) dx' \tag{2.1}$$

where Δ is the filter width.

The governing equations for incompressible flows are the filtered continuity and Navier-Stokes equations

$$\frac{\partial \overline{u}_i}{\partial x_i} = 0 \tag{2.2}$$

$$\frac{\partial \overline{u}_i}{\partial t} + \frac{\partial \overline{u}_i \overline{u}_j}{\partial x_j} = -\frac{\partial \overline{p}}{\partial x_i} + \frac{1}{Re_\tau}\frac{\partial^2 \overline{u}_i}{\partial x_j^2} - \frac{\partial \tau_{ij}}{\partial x_j} \tag{2.3}$$

where u_i denotes velocity vector and x_i the space coordinates. Re_τ is the Reynolds number, t is time, and p is pressure. The SGS stress tensor is defined as $\tau_{ij} = \overline{u_i u_j} - \overline{u}_i \overline{u}_j$. The equations are normalized with the friction velocity u_τ and the channel half width h.

The product $\overline{u}_i \overline{u}_j$ generates wavenumbers that cause aliasing errors and therefore an alternative to the above filtered Navier-Stokes equations is

$$\frac{\partial \overline{u}_i}{\partial t} + \frac{\partial \overline{\overline{u}_i \overline{u}_j}}{\partial x_j} = -\frac{\partial \overline{p}}{\partial x_i} + \frac{1}{Re_\tau}\frac{\partial^2 \overline{u}_i}{\partial x_j^2} - \frac{\partial \overline{\eta}_{ij}}{\partial x_j} \tag{2.4}$$

where $\overline{\eta}_{ij}$ is the SGS stress tensor defined as $\overline{\eta}_{ij} = \overline{u_i u_j} - \overline{\overline{u}_i \overline{u}_j}$. By explicitly filtering the non-linear terms, the wavenumber content of these terms is controlled (Lund 1997). In Eq. (2.4), all the terms of the Navier-Stokes equations contain the same wavenumbers.

The stress tensors τ_{ij} and η_{ij} describe the interaction between the large resolved Grid Scale (GS) and the small unresolved SGS. The stress tensors do not contain the same terms. If decomposition is applied to the velocity correlation $\overline{u_i u_j}$, τ_{ij} can be written as the sum of the Leonard stresses, L_{ij}, the cross stresses, C_{ij}, and the Reynolds stresses, R_{ij}, as $\tau_{ij} = L_{ij} + C_{ij} + R_{ij}$ (Clark *et al.* 1979). The expressions for the stresses are

$$L_{ij} = \overline{\overline{u}_i \overline{u}_j} - \overline{u}_i \overline{u}_j$$

$$C_{ij} = \overline{\overline{u}_i u'_j} + \overline{u'_i \overline{u}_j}$$

$$R_{ij} = \overline{u'_i u'_j}$$

where u'_i is the velocity fluctuation. The expliclit filtering of the convective terms in Eq. (2.4) results in a different expression of the SGS stress $\overline{\eta}_{ij}$. The interaction between the resolved scales, the Leonard stresses, is implicitly included in the convective terms.

The stress tensor is described as the sum of the cross stresses and Reynolds stresses, $\overline{\eta}_{ij} = C_{ij} + R_{ij}$. The SGS stress tensors cannot be expressed in the resolved flow field variables and therefore, they have to be modeled.

2.2. *Subgrid-scale models*

Two widely-used SGS models are the scale similarity model (SSM) proposed by Bardina *et al.* (1980) and the DSM by Germano *et al.* (1991). It has been shown that the SSM does not dissipate enough energy and it is therefore most commonly used in a linear combination with a more-dissipative model such as the Smagorinsky model (Smagorinsky 1963) to form the MM. The model parameter in the Smagorinsky model can be either constant or calculated dynamically during the entire simulation. This is also the case when the Smagorinsky model is used in the MM. Bardina *et al.* (1980) used a constant model parameter while Zang *et al.* (1993) applied the dynamic approach. Both the SSM and the dynamic procedure of the DSM use the assumption that the behavior of the resolved and unresolved stresses is similar.

In the present investigation, τ_{ij} is modeled using the DSM while η_{ij} is modeled using either the DSM or the MM. The DSM models the Reynolds stresses in the SGS stress tensors. The influence of the Leonard stresses in τ_{ij} is investigated. For η_{ij}, the cross stresses are modeled by the SSM ($C_{ij} = \overline{u}_i\overline{u}_j - \overline{\overline{u}}_i\overline{\overline{u}}_j$) in the MM. By using the SSM, the possible drawback of Eq. (2.4) not being Galilean invariant is solved (Speziale 1985). An explicit filtering of η_{ij} is performed to ensure that the SGS terms contain only the desired wavenumbers. The model parameter in the DSM is calculated dynamically in all the simulations. The parameter is averaged in the homogeneous directions and calculated by the least square approximation by Lilly (1992).

3. Explicit filter

A general class of commutative discrete filters applied to nonuniform filter widths was proposed by Vasilyev *et al.* (1998). The procedure applies mapping of the nonuniform grid in physical space onto a uniform grid in computational space where the filtering is performed. The filters are constructed by applying a number of constraints to the filter weights to achieve both commutation and an acceptable filter shape. The filter weights are calculated by forcing the zeroth moment to be one and a number of higher moments to be zero. This determines the order of the commutation error. Other constraints can be added to adjust the filter shape.

In the simulations, two fourth-order commutative filters have been applied: one explicit filter and one test filter. The explicit filter is used when the convective terms and the SGS terms are explicitly filtered in Eq. (2.4). The test filter is used as the second filter in the dynamic procedure when calculating the model parameter in the DSM (Germano *et al.* 1991). The ratio between the test and the explicit filter widths is $\Delta_{test}/\Delta_{exp} = 2$. Between the explicit filter width and the computational cell size, the ratio is $\Delta_{exp}/\Delta_{grid} = 2$.

3.1. *Solution algorithm*

The space derivatives in the governing equations are discretized using a fourth-order finite-difference scheme on a staggered grid. The convective terms are discretized in a skew-symmetric form to ensure conservation of turbulent kinetic energy (Morinishi *et al.* 1998; Vasilyev 2000). The equations are solved with the third-order Runge-Kutta scheme described by Spalart *et al.* (1991). The diffusion term in the wall normal direction is treated implicitly with the Crank-Nicolson scheme to ease the constraint on the time step

of the scheme. The splitting method of Dukowicz & Dvinsky (1992) is used to enforce the solenoidal condition. The resulting discrete Poisson equation for pressure is solved using a pentadiagonal direct matrix solver in the wall-normal direction and a discrete Fourier transform in the homogeneous/periodic directions. Periodic boundary conditions are applied in the streamwise and spanwise directions, while no-slip conditions are applied at the walls. A fixed mean pressure gradient is used in the streamwise direction. An evaluation of the fourth-order conservative scheme is reported in Gullbrand (2000).

4. Turbulent channel flow simulations

The Reynolds number is $Re_\tau = 395$ and the computational domain is $(2\pi h, 2h, \pi h)$ in (x, y, z), where x is the streamwise direction, y the wall normal direction, and z the spanwise direction. Two grid resolutions are used: a standard grid (36,37,36) and a fine grid (72,73,72). The computational grid is stretched in the wall normal direction by a hyperbolic tangent function (Vasilyev 2000). For the standard grid resolution, the streamwise grid size is $\Delta x^+ = 69$, the spanwise grid size $\Delta z^+ = 34$, and in the wall normal direction the grid size varies between $0.5 \leq \Delta y^+ \leq 56$. For the fine grid resolution, the values are $\Delta x^+ = 34$, $\Delta z^+ = 17$, and $0.25 \leq \Delta y^+ \leq 30$. A statistically stationary solution is obtained after 60 dimensionless time units and thereafter statistics are sampled during 30 time units. The time is normalized with the friction velocity and the channel half width.

5. Results

The results from using commutative explicit filtering in LES using the DSM and the MM are compared to the DNS data by Moser *et al.* (1999) for mean velocity, velocity fluctuations and energy spectra. The explicit filtering enters only into the equations through the calculation of the model parameter in the DSM, the second filtering of the velocity field used in the MM, and through the explicit filtering of the convective terms and SGS tensor in Eq. (2.4).

5.1. *Mean velocities*

The mean velocity profile predicted by using the explicit filtering and the DSM is overestimated in the log-law region when compared to the DNS data. The results are somewhat surprising, because the DSM is known to perform better (Gullbrand 2000). However, the model has not previously been applied in turbulent channel flow where three dimensional filtering is employed. The overestimation is not a result of the three dimensionality of the filter. This is shown in Fig. 1. When filtering only in the homogeneous directions is used, the overestimation in the log-law region increases. The overestimation is not an artifact of the relatively coarse resolution either. The fine grid resolution improves the results slightly, but the improvement is not good enough to explained the model behavior.

The explicit filtering of the convective terms and the SGS stress tensor in Eq. (2.4) show only a small influence on the results (Fig. 2). However, the slope in the log-law region is incorrect when explicit filtering are not performed of the previously mentioned terms. Eq. (2.4) produces the correct slope when using the DSM while Eq. (2.3) does not.

The mean velocity profile improves when the MM is used instead of only the DSM in Eq. (2.4). However, the MM also overestimates the log-law region compared to the DNS

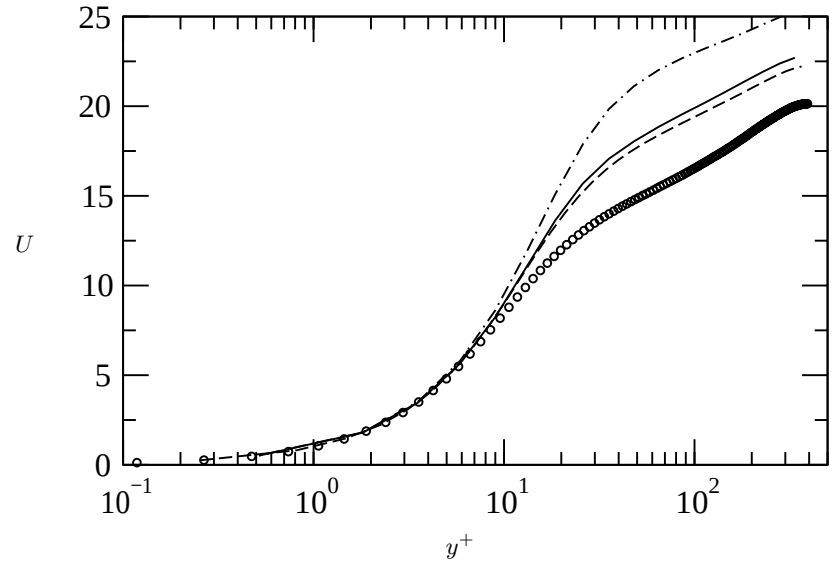

FIGURE 1. Mean velocity profile U as a function of the distance to the wall y^+. ∘: DNS, ——— : Eq. (2.4) with η_{ij} = DSM, - - - - : Eq. (2.4) with η_{ij} = DSM fine grid, and – · – : Eq. (2.4) with η_{ij} = DSM xz-filter.

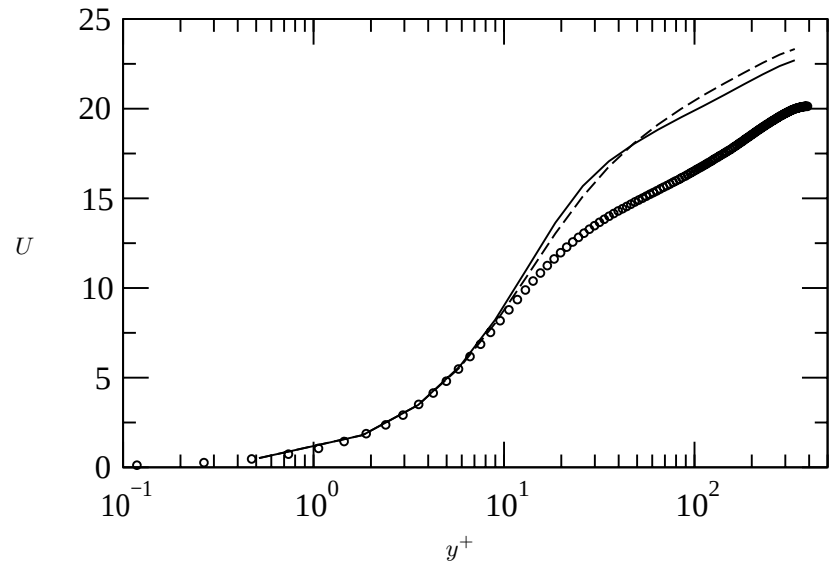

FIGURE 2. Mean velocity profile U as a function of the distance to the wall y^+. ∘: DNS, ——— : Eq. (2.4) with η_{ij} = DSM, and - - - - : Eq. (2.3) with τ_{ij} = DSM.

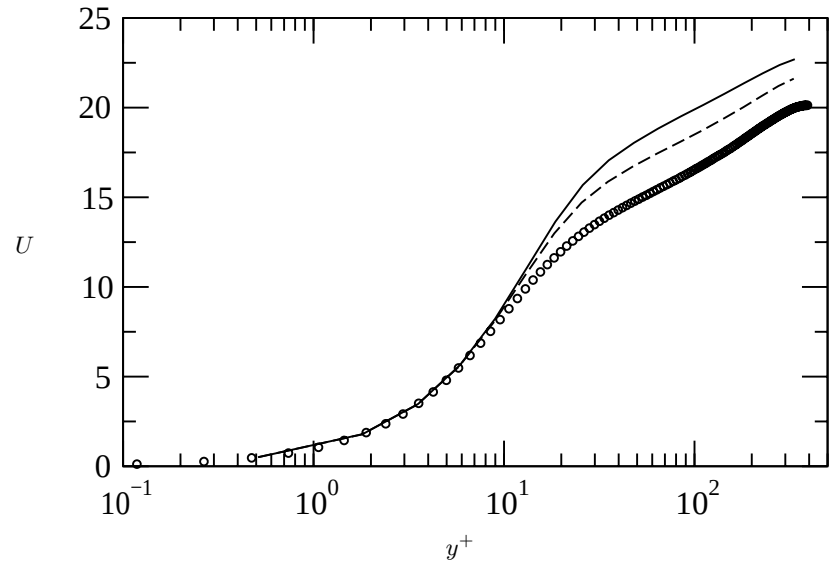

FIGURE 3. Mean velocity profile U as a function of the distance to the wall y^+. ∘: DNS, ——— : Eq. (2.4) with η_{ij} = DSM, and - - - - : Eq. (2.4) with η_{ij} = MM.

data. The overestimation using the MM is about 7 % at the center of the channel while it is 13 % for the DSM. This is shown in Fig. 3.

5.2. *Velocity fluctuations*

The streamwise velocity fluctuation is overpredicted, while the wall normal and spanwise fluctuations are underpredicted when using explicit commutative filters on both the standard and fine computational grids. The difference between the LES and the DNS results is even larger when two dimensional filtering is applied. The predicted peak value in the streamwise direction is reduced on the finer grid (Fig. 4). Usually, the same trend with overprediction of the streamwise fluctuation and underprediction of the other two fluctuations is observed in the commonly used LES approach (Gullbrand 2000).

The velocity fluctuations using Eq. (2.4) are better predicted when compared to Eq. (2.3). The both equations predict equally high peak of the streamwise velocity fluctuation, but the wall normal and spanwise fluctuations are better captured by Eq. (2.4). This is shown in Fig. 5.

A lower peak value of the streamwise velocity fluctuation is predicted when the MM is compared to the DSM. Both results are calculated using Eq. 2.4. The MM results in an overprediction of the peak value of 16 % while it is 40 % for DSM. The wall normal and the spanwise fluctuations are better predicted with the DSM than the MM (Fig. 6).

5.3. *Energy spectra*

The resolved wavenumbers for the standard grid resolution and the fine grid can be seen in Fig. 7, where the energy spectra for each velocity correlation are shown as a function of the streamwise wavenumber. The increased resolution results in resolving higher wavenumbers. The filtering procedure in only the homogeneous directions does not include as broad spectra of resolved wavenumbers compared to filtering in all three

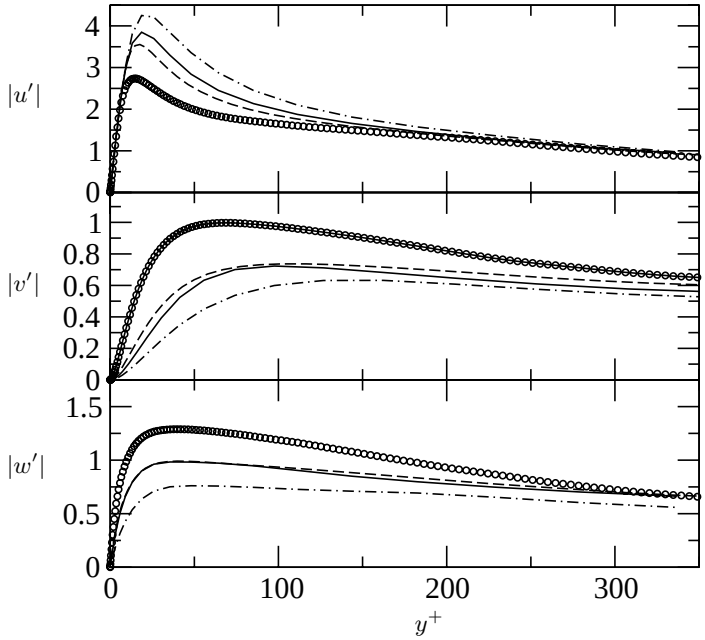

FIGURE 4. Velocity fluctuations in streamwise $|u'|$, wall normal $|v'|$ and spanwise $|w'|$ direction as a function of the distance to the wall y^+. ○: DNS, ——— : Eq. (2.4) with η_{ij} = DSM, - - - - : Eq. (2.4) with η_{ij} = DSM fine grid, and – · – : Eq. (2.4) with η_{ij} = DSM xz-filter.

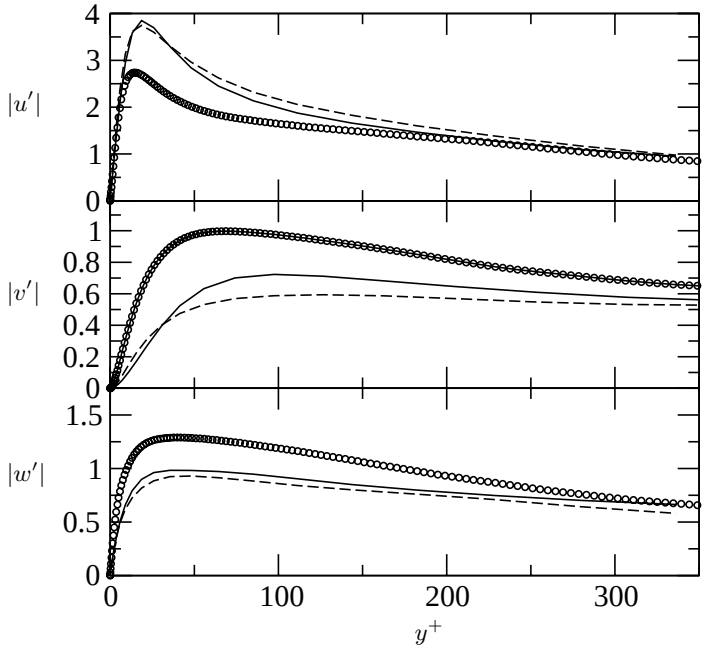

FIGURE 5. Velocity fluctuations in streamwise $|u'|$, wall normal $|v'|$ and spanwise $|w'|$ direction as a function of the distance to the wall y^+. ○: DNS, ——— : Eq. (2.4) with η_{ij} = DSM, and - - - - : Eq. (2.3) with τ_{ij} = DSM.

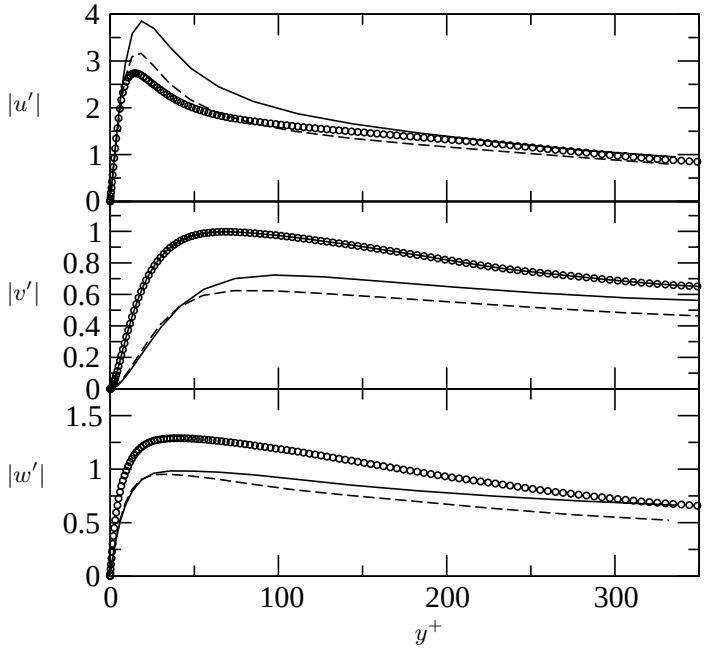

FIGURE 6. Velocity fluctuations in streamwise $|u'|$, wall normal $|v'|$ and spanwise $|w'|$ direction as a function of the distance to the wall y^+. ○: DNS, ——— : Eq. (2.4) with η_{ij} = DSM, and - - - - : Eq. (2.4) with η_{ij} = MM.

dimensions. The fine grid resolution shows better resolution of the small wavenumbers when compared to the DNS results than the standard grid simulations do.

The energy spectra are different for using the DSM in Eq. (2.4) or in Eq. (2.3). Eq. (2.4) results in a higher energy content of the small wavenumbers, while the energy decays also in the small wavenumbers when Eq. (2.3) is employed (Fig. 8).

The MM captures the small wavenumbers better than the DSM. The MM also results in a small increase of the resolved wavenumbers. This is shown in Fig. 9.

The influence of the finite difference scheme on the wavenumbers is clearly seen in the figures. The steep slope at high wavenumbers is due to the modified wavenumber argument (Lund & Kaltenbach 1995).

6. Discussion and conclusions

Three dimensional explicit filtering in LES has been used for the DSM and the MM in turbulent channel flow. The simulations were performed using fourth order conservative finite difference schemes. The three dimensional explicit filter functions commute up to fourth order. The result of performing LES using the commutative filters is that the mean velocity profile is overestimated in the log-law region. The overestimation is not a result of the introduction of filtering in the wall normal direction. According to Fig. 1, the overestimation becomes even larger when filtering is applied only in the homogeneous directions.

The two formulations of the Navier-Stokes equations, Eq. (2.3) and Eq. (2.4), predict slightly different results. Eq. (2.4) has the best behavior and also the most consistent approach, with all the terms in the equation containing the same wavenumbers. This

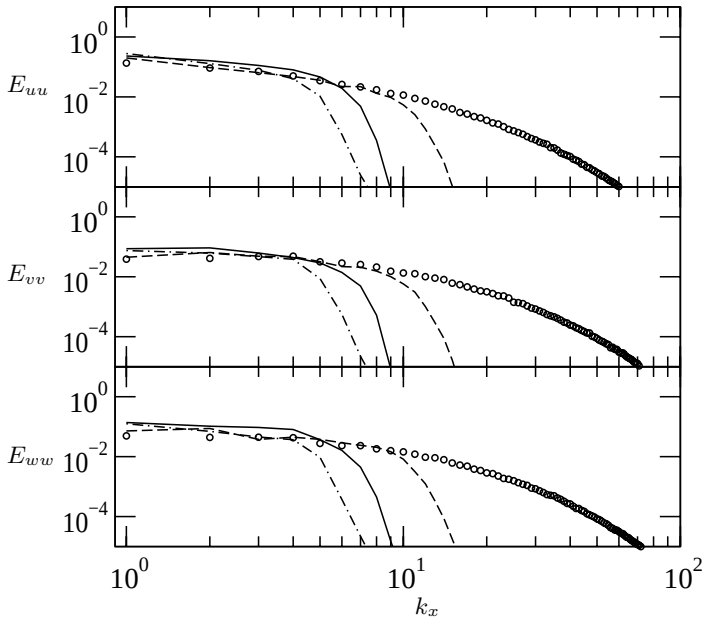

FIGURE 7. Energy spectrum of the streamwise E_{uu}, wall normal E_{vv} and spanwise E_{ww} velocity correlation as a function of the streamwise wavenumber k_x at $y^+ \approx 395$. ∘: DNS, ——— : Eq. (2.4) with η_{ij} = DSM, - - - - : Eq. (2.4) with η_{ij} = DSM fine grid, and – · – · –: Eq. (2.4) with η_{ij} = DSM xz-filter.

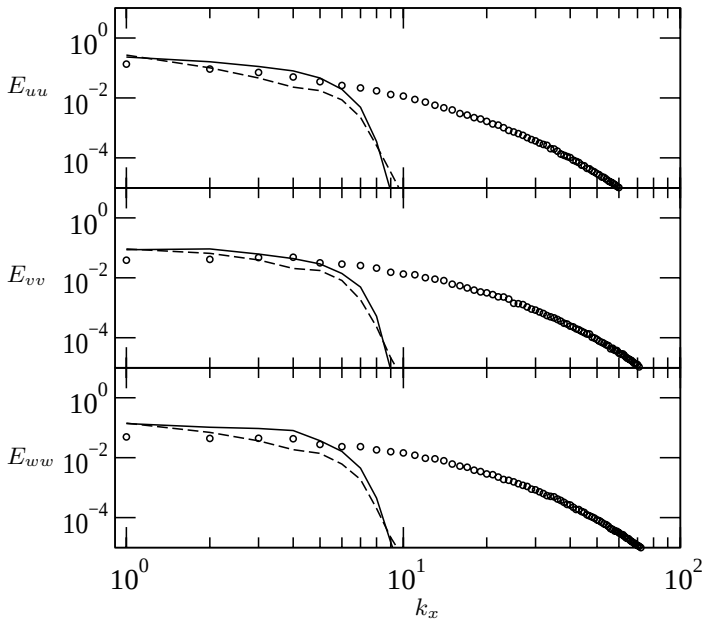

FIGURE 8. Energy spectrum of the streamwise E_{uu}, wall normal E_{vv} and spanwise E_{ww} velocity correlation as a function of the streamwise wavenumber k_x at $y^+ \approx 395$. ∘: DNS, ——— : Eq. (2.4) with η_{ij} = DSM, and - - - - : Eq. (2.3) with τ_{ij} = DSM.

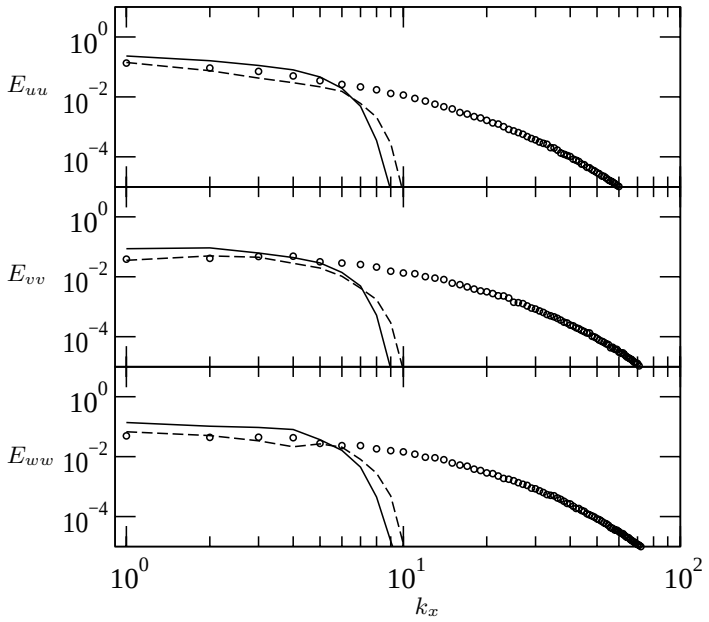

FIGURE 9. Energy spectrum of the streamwise E_{uu}, wall normal E_{vv} and spanwise E_{ww} velocity correlation as a function of the streamwise wavenumber k_x at $y^+ \approx 395$. ○: DNS, ——— : Eq. (2.4) with η_{ij} = DSM, and - - - - : Eq. (2.4) with η_{ij} = MM.

is achieved by explicitly filtering the convective terms and the SGS stress tensor. By filtering the convective terms, the Leonard stress term is accounted for in the equation. The difference in the calculated results between Eq. (2.3) and Eq. (2.4) is due to the influence of the Leonard stress tensor.

The MM captures the large scale behavior better that the DSM. This result depends upon the shape of the filter function. Most simulations with the DSM have been performed using the sharp cut-off filter in the homogeneous directions as the test filter. The developed commutative filters are Gaussian like filters. A study by Piomelli *et al.* (1988) showed that for two dimensional filtering, the best results are obtained by using the Gaussian filter with the MM and the cut-off filter with the Smagorinsky model. The Gaussian filter used in the Smagorinsky model resulted in an overprediction of the mean velocity profile in the log-law region. The over-prediction was about 17 % at the center of the channel for $Re_\tau = 180$. The findings by Piomelli *et al.* (1988) are confirmed in this study in Fig. 10. The commonly used LES approach without explicit filtering has been performed and two different test filters have been used: the commutative filter and the sharp cut-off filter. The standard grid resolution was used in the simulations. The filters are only employed in the homogeneous directions and the filter widths are twice the computational grid size. The test filters enter into the equations only through the calculation of the model parameter in the DSM. The mean velocity profiles are shown in Fig. 10. The velocity profile is highly overpredicted in the log-law region when using the commutative filter when compared to the results from using the sharp cut-off filter.

The contribution from the SGS model is increased in the explicitly filtered LES compared to the commonly used LES approach. The increase is expected, due to a reduction or an elimination of the high wavenumbers by the filtering procedure, causing the SGS

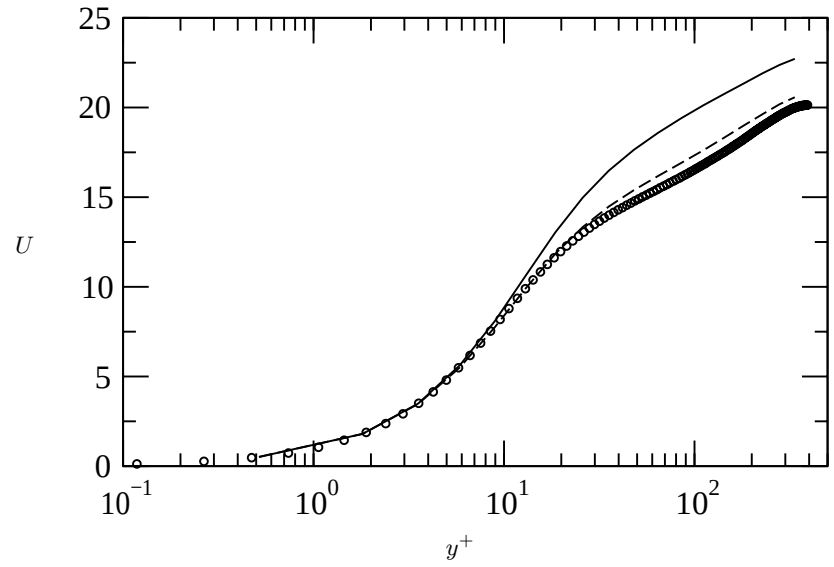

FIGURE 10. Mean velocity profile U as a function of the distance to the wall y^+. ○: DNS, ——— : DSM 2-D commutative filter, and – – – – : DSM 2-D sharp cut-off filter.

model to model a larger range of wavenumbers. Therefore, the SGS model has a larger influence in the explicitly filtered LES.

7. Current work

In the current work, the true LES approach is investigated. The true LES is obtained by keeping the explicit filter width constant while the computational grid is refined. The solution converges to a true LES.

Different SGS models will also be investigated as well as the numerical error in the simulation. Two promising SGS models that have proven to perform well are the multi-scale model by Hughes *et al.* (2001) and the approximate deconvolution model by Stolz *et al.* (2001). The LES of turbulent channel flow in both papers have been performed using spectral methods. The models will be applied in the previously discussed fourth order finite difference code.

Acknowledgments

The author wishes to thank Prof. O. V. Vasilyev for providing the channel flow code and Prof. P. Moin for many helpful discussions. Discussions with Dr. Y. Dubief and Mr. G. Iaccarino are also gratefully acknowledged.

REFERENCES

BARDINA, J., FERZIGER, J. H. & REYNOLDS, W. C. 1980 Improved subgrid scale models for large eddy simulation. *AIAA-80-1357*.

CLARK, A., FERZIGER, J. H. & REYNOLDS, W. C. 1979 Evaluation of subgrid-scale models using an accurately simulated turbulent flow. *J. Fluid Mech.*, **91**, 1-16.

Dukowicz, J. K. & Dvinsky, A. S. 1992 Approximation as a higher order splitting for the implicit incompressible flow equations. *J. Comp. Phys.*, **102**, 336-347.

Germano, M., Piomelli, U., Moin, P. & Cabot, W. H. 1991 A dynamic subgrid-scale eddy viscosity model. *Phys. Fluids A.* **3**, 1760-1765.

Ghosal, S. 1995 An analysis of numerical errors in large-eddy simulations of turbulence. *J. Comp. Phys.* **125**, 187-206.

Ghosal, S. & Moin, P. 1995 The basic equations of the large eddy simulation of turbulent flows in complex geometry. *J. Comp. Phys.* **118**, 24-37.

Gullbrand, J. 2000 An evaluation of a conservative fourth order DNS code in turbulent channel flow. *Annual Research Briefs*, Center for Turbulence Research, NASA Ames/Stanford Univ. 211-218.

Hughes, T. J. R., Oberai, A. A. and Mazzei, L. 2001 Large eddy simulation of turbulent chennel flows by the variational multiscale method. *Phys. Fluids*, **13**, 1784-1799.

Lilly, D. K. 1992 A proposed modification of the Germano subgrid-scale closure method. *Phys. Fluids A.* **4**, 633-635.

Lund, T. S. 1997 On the use of discrete filters for large eddy simulation. *Annual Research Briefs*, Center for Turbulence Research, NASA Ames/Stanford Univ. 83-95.

Lund, T. S. & Kaltenbach, H.-J. 1995 Experiments with explicit filtering for LES using a finite-difference method. *Center for Turbulence Research, Annual Research Briefs 1995*, 91-105.

Morinishi, Y., Lund, T. S., Vasilyev, O. V. & Moin, P. 1998 Fully conservative higher order finite difference schemes for incompressible flow. *J. Comp. Phys.* **143**, 90-124.

Moser, R. D., Kim, J. & Mansour, N. N. 1999 Direct numerical simulation of turbulent channel flow up to Re_τ=590. *Phys. Fluids.* **11**, 943-945.

Najjar, F. M. & Tafti, D. K. 1996 Study of discrete test filters and finite difference approximations for the dynamic subgrid-scale stress model. *Phys. Fluids.* **8**, 1076-1088.

Piomelli, U., Moin, P. & Ferziger, J. H. 1988 Model consistency in large eddy simulation of turbulent channel flows. *Phys. Fluids.* **31**, 1884-1891.

Smagorinsky, J. 1963 General circulation experiments with the primitive equations. *Mon. Weather Rev.* **91**, 99-152.

Spalart, P., Moser, R. & Rogers, M. 1991 Spectral methods for the Navier-Stokes equations with one infinite and two periodic directions. *J. Comp. Phys.* **96**, 297-324.

Speziale, C. G. 1985 Galilean invariance of subgrid-scale stress models in the large-eddy simulation of turbulence. *J. Fluid Mech.* , 55-62.

Stolz, S., Adams, N. A. & Kleiser, L. 2001 An approximate deconvolution model for large-eddy simulation with application to incompressible wall-bounded flows. *Phys. Fluids.* **13**, 997-1015.

Vasilyev, O. V. 2000 High order finite difference schemes on non-uniform meshes with good conservation properties. *J. Comp. Phys.* **157**, 746-761.

Vasilyev, O. V., Lund, T. S. & Moin, P. 1998 A general class of commutative filters for LES in complex geometries. *J. Comp. Phys.* **146**, 82-104.

Zang, Y., Street, R. L. & Koseff, J. R. 1993 A dynamic mixed subgrid-scale model and its application to turbulent recirculating flows. *Phys. Fluids.* **5**, 3186-3196.